Analysis and Damping Enhancement Method for Air Conditioning Load Recovery in Weak Power Grid

Bowen Zheng
China Electric Power Research Institute
Beijing, China
bw.zheng@outlook.com

Chang Liu
China Electric Power Research Institute
Beijing, China
liuchang3@epri.sgcc.com.cn

Mingming Pan
China Electric Power Research Institute
Beijing, China
panmingming1@epri.sgcc.com.cn

Jing Zhang
China Electric Power Research Institute
Beijing, China
zhangjing8@epri.sgcc.com.cn

Feixiang Gong
China Electric Power Research Institute
Beijing, China
gongfeixiang@epri.sgcc.com.cn

Yongjun Li
China Electric Power Research Institute
Beijing, China
liyongjun@epri.sgcc.com.cn

Jindou Yuan
China Electric Power Research Institute
Beijing, China
yuanjd@epri.sgcc.com.cn

Zishang Xu
China Electric Power Research Institute
Beijing, China
xuzishang@epri.sgcc.com.cn

***Abstract*—To address the harmonic resonance issues induced by rapid grid-load impedance interaction during air-conditioning (AC) load recovery in weak-grid scenarios, this paper constructs an AC load impedance model incorporating variable-frequency compressors, AC/AC converters, and control loops. Based on the grid-load system impedance model, the positive resonance-inducing effects of increasing AC load switching units and abrupt power recovery during load restoration are analyzed. A damping enhancement control scheme is proposed by leveraging the resonance-cancellation mechanism of an equivalent series negative inductance and a positive resistance. Hardware-in-the-loop experiments validate the proposed method's feasibility, demonstrating effective suppression of harmonic resonance during flexible power recovery. The results indicate improved grid security during multi-mode AC load recovery.**

***Keywords*—Air-conditioning (AC); load recovery; weak grid; resonance; damping enhancement**

I. Introduction

In the context of the transformation of the new-type power system and energy structure, air conditioning load, as a core component of the power grid's peak load, has become a key link in achieving the "dual carbon" goal through the exploration of its controllable potential and safe regulation. Air conditioning cooling load is mainly provided by the compressor, which is controlled by a power electronic converter. During the load recovery process, in addition to the above-mentioned issues of cold start load surge, communication reliability requirements, and distribution network voltage and frequency safety, the time-varying characteristics of the short-circuit ratio of the weak power grid under the background of the new distribution network and the rapid interaction of grid-load impedance caused by the high proportion of power electronic devices give rise to new problems of power load resonance.

In recent years, relevant research has provided important insights into the safety and stability issues of air conditioning loads participating in system regulation and recovery processes. In terms of air conditioning load aggregation control, studies such as [1] have developed a two-layer control framework to evaluate air conditioning response potential across multiple factors, providing a theoretical basis for load-side resources to participate in optimal scheduling. In terms of control strategies, [2] proposed frequency regulation by adjusting the temperature setpoint. This type of flexible control not only ensured user comfort but also provided a practical means for safely controlling the load recovery process. With the increasing penetration rate of power electronic equipment in the distribution system, load modeling and stability analysis have become particularly important. [3] used the D-Q impedance modeling method to analyze the stability of a three-phase four-wire system with a single-phase load, providing a methodological reference for establishing an overall impedance model of air conditioning load, including converters, and analyzing the resonance characteristics of weak power grids. Regarding resonance suppression, the virtual impedance reshaping technique proposed in [4] achieved decoupling suppression of series resonance and harmonic load current, providing an advanced solution to alleviate harmonic resonance problems during air conditioning load recovery. Meanwhile, the intelligent load coordination control strategy based on electric springs in [5] demonstrated the feasibility of multi-objective coordinated control, providing a new approach for simultaneously achieving frequency regulation and transient voltage recovery.

Existing research has limitations in air-conditioning load modeling and in the analysis of weak-grid resonance characteristics. To address this, this paper establishes an air conditioning load impedance model that incorporates the compressor and frequency converter, analyzes the resonance characteristics during power recovery under weak-grid conditions, and proposes a damping enhancement scheme based on a series equivalent impedance. This scheme can effectively suppress potential harmonic resonances in multi-mode recovery and improve grid operation safety.

XXX-X-XXXX-XXXX-X/XX/$XX.00 ©20XX IEEE
979-8-3315-8138-1

II. IMPEDANCE MODELING OF GRID-CONNECTED SYSTEM WITH AIR CONDITIONING LOAD

A. *Air conditioning load grid-connected system*

The core refrigeration device of the air conditioner is the compressor, which compresses the low-temperature, low-pressure refrigerant gas, raising its temperature and pressure to power the refrigerant cycle and drive the heat exchange process of the entire air conditioning system. The inverter compressor system of the inverter air conditioner can be equivalent to a closed-loop control system of a permanent magnet synchronous motor driven by an inverter. Its core is to convert power-frequency alternating current into a variable-frequency power supply via a frequency converter to drive a compressor motor with a built-in permanent-magnet rotor. The frequency converter dynamically adjusts the output frequency (corresponding to the motor speed) according to the feedback of the temperature sensor, realizes the stepless adjustment of the cooling capacity, dynamically matches the cooling demand, reduces the energy consumption by running at low speed under low load, and outputs the strong cooling effect at high speed under high load. The schematic diagram of the grid-connected air conditioning load system is shown in Fig. 1.

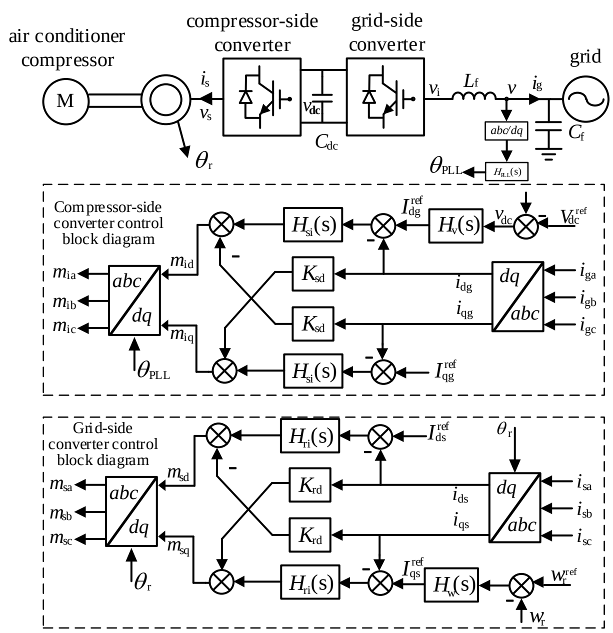

Fig.1 Schematic diagram of air conditioning load grid-connected system

B. *Impedance modeling of air conditioning load device*

1) Modeling of admittance matrix based on harmonic linearization

The driving system of the permanent magnet synchronous compressor consists of a mechanical subsystem and an electrical subsystem. The mechanical subsystem uses the compressor as its core and connects the rotor of the permanent magnet synchronous motor (PMSM) via an elastic coupling shaft. The electrical subsystem includes the back-to-back converter (the former PFC part and the latter electric drive part), the DC bus, and the filter circuit.

Based on the harmonic linearization method, a small signal disturbance with frequency f_p is injected into the DC bus voltage at the steady-state operating point corresponding to the fundamental frequency $\Delta V_{dc}(f_p)$. This perturbation can be expressed in the complex form $\Delta V_{dc}(f_p) = |\Delta V_{dc}|e^{j\emptyset v}$, of which $|\Delta V_{dc}|$ and $\emptyset_v$ amplitude and phase, respectively. Due to the nonlinear characteristics of the space vector pulse width modulation (SVPWM) and the asymmetric response of the *dq*-axis current controller, when a disturbance is injected, a frequency of will be simultaneously generated in the converter output current f_p positive sequence harmonics of $\Delta I_P(f_p)$ and the frequency is $f_n = 2f_0 - f_p$ negative sequence harmonics of $\Delta I_n(f_n)$. This phenomenon is defined as the frequency coupling effect. The transfer relationships of the above harmonic components can be represented in matrix form, and the harmonic matrices for the DC bus voltage, converter output voltage, and current are shown in Eqn. (1):

$$\mathbf{v}_{\mathrm{a}} = \begin{bmatrix} \hat{V}_{\mathrm{p}}(f_{\mathrm{p}}) \\ \hat{V}_{\mathrm{n}}(f_{\mathrm{n}}) \end{bmatrix}, \quad \mathbf{v}_{\mathrm{ia}} = \begin{bmatrix} \hat{V}_{\mathrm{ip}}(f_{\mathrm{p}}) \\ \hat{V}_{\mathrm{in}}(f_{\mathrm{n}}) \end{bmatrix}, \quad \hat{\mathbf{i}}_{\mathrm{ga}} = \begin{bmatrix} \hat{I}_{\mathrm{gp}}(f_{\mathrm{p}}) \\ \hat{I}_{\mathrm{gn}}(f_{\mathrm{n}}) \end{bmatrix} \tag{1}$$

Power harmonics can be transferred to the DC bus, resulting in harmonics on the DC bus of $\Delta V_{dc}(f_p - f_1)$. Due to the rotor flux-oriented control strategy and the DC bus voltage harmonics, the output voltage and current of the converter will contain a frequency of $f_p - f_1 + f_r$ and $f_p - f_1 - f_r$, as shown in Eqn. (2):

$$\mathbf{v}_{\mathrm{sa}} = \begin{bmatrix} \hat{V}_{\mathrm{sp}}\left(f_{\mathrm{p}} - f_1 + f_{\mathrm{r}}\right) \\ \hat{V}_{\mathrm{sn}}\left(f_{\mathrm{p}} - f_1 - f_{\mathrm{r}}\right) \end{bmatrix}, \quad \hat{\mathbf{i}}_{\mathrm{sa}} = \begin{bmatrix} \hat{I}_{\mathrm{sp}}\left(f_{\mathrm{p}} - f_1 + f_{\mathrm{r}}\right) \\ \hat{I}_{\mathrm{sn}}\left(f_{\mathrm{p}} - f_1 - f_{\mathrm{r}}\right) \end{bmatrix} \tag{2}$$

Therefore, the relationship between the voltage and current harmonics at the air conditioning load grid-connected point can be expressed as:

$$Y \cdot \hat{v}_a = -\hat{i}_{ga} \tag{3}$$

where Y is the required admittance.

2) Dynamic modeling of an air conditioning compressor

The mechanical shafting structure of the air conditioning compressor drive system is composed mainly of a permanent-magnet synchronous motor rotor, a compressor impeller, and a rigid shaft connecting them. The electromagnetic torque output by the motor is transmitted to the compressor impeller via the shafting, driving it to rotate and enabling refrigerant compression. At the same time, the load torque generated during the compressor's working process acts on the shafting, resulting in a two-way torque interaction.

To simplify the analysis of the shafting's dynamic characteristics, the shaft connecting the motor rotor and the compressor impeller is modeled as a torsional spring with elastic and damping properties. In contrast, the motor rotor and the compressor impeller are treated as rigid masses. Based on this, the mechanical shafting studied in this paper is modeled by a double-mass-spring model:

979-8-3315-8138-1

$$\begin{cases} J_1 \dfrac{d\omega_1}{dt} = T_m - T_{em} \\ J_2 \dfrac{d\omega_2}{dt} = T_{em} + T_e \\ T_{em} = D(\omega_1 - \omega_2) + K(\theta_1 - \theta_2) \end{cases} \tag{4}$$

where J_1 and J_2 are the inertia of the compressor impeller and rotor, K and D are the stiffness and damping coefficients of the shafting, and T_m and T_e are the mechanical torque and electromagnetic torque.

When the system is in steady state, the relative angular displacement between the motor rotor and the compressor impeller is constant, maintained by the balance of electromagnetic torque, load torque, and shafting coupling torque. A small signal disturbance on the DC bus causes a small fluctuation in electromagnetic torque, breaking the original torque balance. The imbalance leads to small disturbances $\Delta\theta_1$ and $\Delta\theta_2$ in the angular positions of the two masses, and their relative changes will cause the torsional vibration of the shafting. The corresponding small-signal perturbation model is as follows:

$$\begin{cases} s^2 J_1 \hat{\theta}_1 = \hat{T}_{\mathrm{m}} - \hat{T}_{\mathrm{em}} \\ s^2 J_2 \hat{\theta}_2 = \hat{T}_{\mathrm{e}} + \hat{T}_{\mathrm{em}} \\ \hat{T}_{\mathrm{em}} = (Ds + K)\left(\hat{\theta}_1 - \hat{\theta}_2\right) \end{cases} \tag{5}$$

The frequency-domain expression can be obtained by applying the Laplace transform to Eqn. (5):

$$\begin{cases} \hat{\theta}_1 = M_1(s)\hat{\theta}_2 \\ \hat{T}_{\mathrm{e}} = M(s)\hat{\theta}_2 \end{cases} \tag{6}$$

where the transmission system dynamic transfer function of the coupling shaft is:

$$\begin{aligned} M_1(s) &= \frac{Ds + K}{J_1 s^2 + Ds + K} \\ M(s) &= \left(J_2 s^2 + Ds + K\right) - \frac{(Ds + K)^2}{J_1 s^2 + Ds + K} \end{aligned} \tag{7}$$

3) Electromagnetic model of an air conditioning compressor

In the three-phase steady-state coordinate system, the stator voltage equation and the flux linkage equation of the air conditioning compressor motor are expressed as:

$$\begin{cases} v_{\mathrm{sa}} = R_{\mathrm{s}} i_{\mathrm{sa}} + \dfrac{d\psi_{\mathrm{a}}}{dt} \\ v_{\mathrm{sb}} = R_{\mathrm{s}} i_{\mathrm{sb}} + \dfrac{d\psi_b}{dt} \\ v_{\mathrm{sc}} = R_{\mathrm{s}} i_{\mathrm{sc}} + \dfrac{d\psi_c}{dt} \end{cases} \tag{8}$$

$$\begin{bmatrix} \psi_{\mathrm{a}} \\ \psi_{\mathrm{b}} \\ \psi_{\mathrm{c}} \end{bmatrix} = \begin{bmatrix} L_{\mathrm{aa}} & L_{\mathrm{ab}} & L_{\mathrm{ac}} \\ L_{\mathrm{ba}} & L_{\mathrm{bb}} & L_{\mathrm{bc}} \\ L_{\mathrm{ca}} & L_{\mathrm{cb}} & L_{\mathrm{cc}} \end{bmatrix} \begin{bmatrix} i_{\mathrm{sa}} \\ i_{\mathrm{sb}} \\ i_{\mathrm{sc}} \end{bmatrix} + \begin{bmatrix} \psi_{\mathrm{am}} \\ \psi_{\mathrm{bm}} \\ \psi_{\mathrm{cm}} \end{bmatrix} \tag{9}$$

where R_s is the resistance of each phase winding of the stator, Ψ_{a}, Ψ_{b} and Ψ_{c} are the three-phase stator flux linkage, Ψ_{am}, Ψ_{bm} and Ψ_{cm} are the projections of the permanent magnet flux linkage on each phase winding, L_{aa}, L_{bb}, and L_{cc} are the self-inductances of the stator phase windings, and L_{ab}, L_{ac}, L_{ba}, L_{bc}, L_{ca}, L_{cb} are the mutual inductances between the phases.

The electromagnetic torque can be expressed in the time domain as:

$$T_{\mathrm{e}} = 1.5p\left[\psi_{\mathrm{m}} i_{\mathrm{qs}} + (L_{\mathrm{d}} - L_{\mathrm{q}}) i_{\mathrm{ds}} i_{\mathrm{qs}}\right] \tag{10}$$

where L_{d} and L_{q} are the stator inductances along the DQ axis, respectively.

The voltage and flux linkage equations of the air conditioner compressor are transformed using the symmetrical component method. A small-signal linear model including voltage harmonics, current harmonics, and rotor angle position disturbance can be established, and the specific form is as follows:

$$\mathbf{G}_1 \hat{\mathrm{v}}_{\mathrm{sa}} = \mathbf{G}_2 \hat{\mathbf{i}}_{\mathrm{sa}} + \mathbf{G}_3 \hat{\theta}_{\mathrm{r}} \tag{11}$$

Due to the electromagnetic torque disturbance caused by the stator current harmonics acting on the rotor mass block, the electrical angle position disturbance will be generated. The relationship between the rotor mechanical angular position disturbance and the stator current harmonics can be established by combining the small-signal disturbance of the electromagnetic torque in Eqns. (10) and (11) with the Park transform and the inverse Park transform. This relationship can be stated as follows:

$$\hat{\theta}_{\mathrm{r}} = \mathbf{T}\hat{\mathbf{i}}_{\mathrm{sa}} \tag{12}$$

4) State space modeling of the converter system

The overall system structure includes the compressor load, rotor, back-to-back PWM converter (including the machine-side electric drive converter MSC and the grid-side power factor correction PFC converter GSC), and a DC bus connected to the grid. The MSC generates a modulation signal through a speed loop and a current loop to drive the compressor group. In contrast, the GSC controller maintains a constant DC bus voltage and ensures balanced power flow between the GSC and the MSC. The transfer function of the phase-locked loop and the closed-loop transfer function of the system are:

$$H_{\mathrm{PLL}}(s) = \left(K_{\mathrm{pp}} + \frac{K_{\mathrm{pi}}}{s}\right)\frac{1}{s} \tag{13}$$

$$T_{\mathrm{PLL}}(s) = \frac{H_{\mathrm{PLL}}(s)}{1 + V_1 H_{\mathrm{PLL}}(s)} \tag{14}$$

The converter is connected to the power grid through the LC filter, and the current transient equation of the filter inductor, the

979-8-3315-8138-1

voltage transient equation of the filter capacitor, the output voltage characteristic equation of the converter, and the DC bus power-voltage dynamic equation can be obtained as follows:

$$\begin{cases} L_{\mathrm{f}}\dfrac{di_{\mathrm{fa}}}{dt}=v_{\mathrm{ia}}-v_{\mathrm{a}}, \\ C_{\mathrm{f}}\dfrac{dv_{\mathrm{a}}}{dt}=i_{\mathrm{fa}}-i_{\mathrm{ga}}, \\ v_{\mathrm{ia}}=K_{\mathrm{m}}v_{\mathrm{dc}}m_{\mathrm{ia}}, \\ v_{\mathrm{sa}}=K_{\mathrm{m}}v_{\mathrm{dc}}m_{\mathrm{sa}}, \\ C_{\mathrm{dc}}\dfrac{dv_{\mathrm{dc}}}{dt}v_{\mathrm{dc}}=\sum\limits_{n=\mathrm{a,b,c}}\left(-v_{\mathrm{sn}}i_{\mathrm{sn}}-v_{\mathrm{in}}i_{n}\right) \end{cases} \tag{15}$$

where L_f is the filter inductor, C_f is the filter capacitor, I_{fa} is the A-phase current of the filter inductor, V_{ia} is the A-phase output voltage of the converter, V_a is the A-phase voltage at the grid side, I_{ga} is the A-phase current at the load side, K_m is the modulation factor, M_{ia} is the A-phase modulation wave of GSC, m_{sa} is the A-phase modulation wave of MSC, V_{dc} is the DC bus voltage, V_{sn} and I_{sn} are the n-phase voltage and current at the grid side (GSC side), V_{in} and I_n are the n-phase voltage and current at the generator side (MSC side).

5) Grid equivalent impedance modeling

The long transmission line and the transformer leakage inductance at the grid side exhibit inductive equivalent impedance characteristics, and the inductive effect is enhanced as the grid-connected capacity of the local new energy increases. The grid-side equivalent impedance expression of the grid-connected system with air conditioning load is as follows:

$$Z_{\mathrm{g}}=sL_{\mathrm{g}}+R_{\mathrm{g}} \tag{16}$$

where, L_g and R_g are respectively the equivalent inductance and equivalent resistance of the grid side impedance of the grid-connected system with air conditioning load.

III. AIR CONDITIONING LOAD DAMPING ENHANCEMENT SCHEMA

To avoid the above resonance problem, a real damping element can be connected in series at the point of connection of the air conditioning load to suppress resonance. At the same time, to avoid the influence of the equivalent parasitic inductance on the grid side of the weak current grid, the offset of the equivalent inductance characteristics on the grid side can be realized by adding a negative virtual inductance. The actual circuit schematic diagram of the series-damping fusion negative virtual inductance is shown in Fig. 2(a). To realize equivalent control of the real circuit, virtual control equivalence can be implemented in the air conditioning load control loop, and the equivalent control block diagram on the network side is shown in Fig. 2(b).

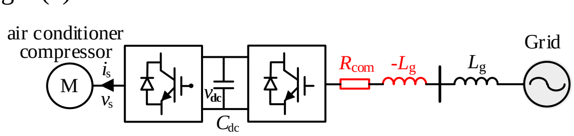

(a) Actual circuit with negative virtual inductance fused by series damping

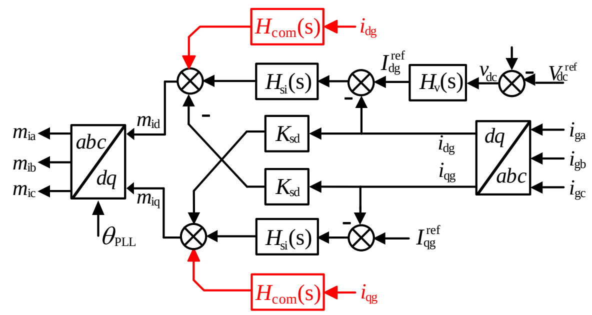

(b) Equivalent control loop of line-side PFC converter

Fig. 2 Principle block diagram of the series damping enhancement scheme

In Fig. 2, the compensation transfer function expression of the feedforward link of the damping enhancement scheme is:

$$H_{\mathrm{com}}=-sL_{\mathrm{g}}+R_{\mathrm{com}} \tag{17}$$

where $-L_g$ is the negative inductance of the equivalent series connection, which is the same as the equivalent inductance of the line side, R_{com} is the damping of the equivalent series connection.

The impedance model of air conditioning load after adopting the improved scheme is:

$$\mathbf{Y}=\mathbf{C}+\frac{\mathbf{E}-\left(\mathbf{P}_1\mathbf{E}_1+\mathbf{P}_3+\mathbf{H}_{\mathrm{com}}\right)-\mathbf{\Gamma}\mathbf{Q}_1\mathbf{E}_1}{\mathbf{L}-\left(\mathbf{P}_1\mathbf{E}_1\mathbf{L}+\mathbf{P}_1\mathbf{E}_2+\mathbf{P}_2\right)-\mathbf{\Gamma}\left(\mathbf{Q}_1\mathbf{E}_1\mathbf{L}+\mathbf{Q}_1\mathbf{E}_2\right)} \tag{18}$$

IV. HARDWARE-IN-THE-LOOP VERIFICATION

Build a hardware-in-the-loop verification platform in the RTDS real-time digital simulation system shown in Fig. 3. The effectiveness of the scheme studied in the previous section is verified by real-time simulation. The system parameters are shown in Table 1.

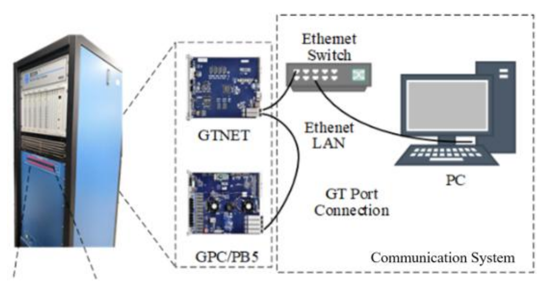

Fig. 3 Hardware-in-the-loop simulation platform

Table 1 System parameters

Type	Parameter value
DC bus capacitance	24000uF
Filter inductance	750uH
Filter capacitor	60uF
Rated frequency of the compressor	50Hz
Inertia time constant of the compressor rotor	0.86s
Damping coefficient	1.4pu
Stiffness of shafting	1.1pu
GSC Current Controller Proportional	0.01
GSC Current Controller Integral	0.62
GSC Voltage Controller Proportioning	1.2
GSC Voltage Controller Integral	30
MSC Current Controller Proportion	1
MSC Current Controller Integral	10

979-8-3315-8138-1

When the air conditioning load participates flexibly in the power grid's demand response by reducing part of its load, it must be restored from the regulated power to the rated operating power after the demand response ends. The air conditioning load uses a conventional control scheme, and the voltage and current waveforms at the grid-connected point for 20 air conditioners under different air conditioning load power recovery conditions are shown in Fig. 4.

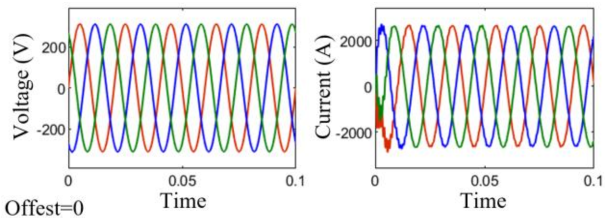

(a) Operating power of 60 kW

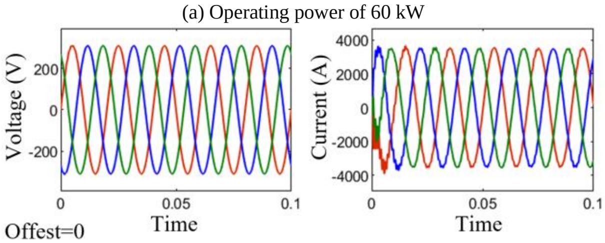

(b) Operating power restored to 80 kW

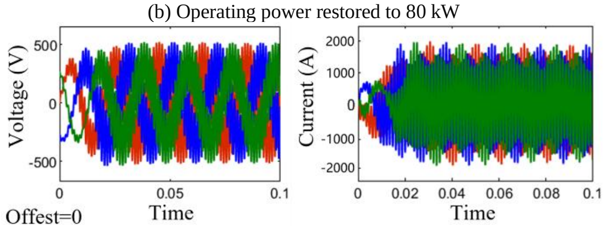

(c) Recovery of operating power to 100 kW

Fig. 4 Voltage and current waveforms at the grid-connected point under different recovery powers of conventional control

It can be seen from Fig. 4 that in the process of recovering the air-conditioning load of the weak grid from the regulated power to the rated operating power, when the operating power of the load of 20 air conditioners is 60kW ~ 80kW, the voltage and current waveforms at the grid-connected point of the air-conditioning load cluster shown in Fig. 4(a) ~ (b) are sinusoidal, and the system can operate stably. When the operating power of the air conditioning load is restored to 100 kW, the voltage and current waveforms at the grid-connected point of the air conditioning load cluster in Fig. 4(c) exhibit resonant behavior, and system stability worsens.

Further, when the air-conditioning load of the weak grid is recovered from the regulated power to the rated operating power, the air-conditioning load adopts the damping enhancement scheme. When the operating power of the load monomer in the load cluster of 20 air conditioners is recovered to the rated power of 120kW, the voltage and current waveforms at the grid-connected point are shown in Fig. 5. It can be seen that the voltage and current waveform of the cluster grid-connected point is sinusoidal after adopting the improved scheme, and the system can operate stably.

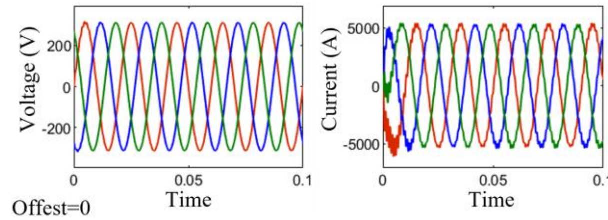

Fig.5 Voltage and current waveforms at PCC under enhanced control

V. Conclusion

In this paper, a harmonic linearization impedance model for a grid-connected system with air-conditioning loads, including power conversion devices and compressors, is established. The evolution characteristics of power quality deterioration at the potential grid-connected point during air conditioning load recovery in a weak grid are analyzed. The positive induction mechanism, revealed by the step change in recovery power during weak-grid resonance, is shown. A scheme for a damping enhancement loop, equivalent to the actual circuit with a negative inductance and a positive resistance in series, is proposed. The scheme is implemented using software control without additional sensors or damping devices. Active impedance matching between the network and the load is achieved by adjusting the converter's output impedance via an extra control loop. The hardware-in-the-loop verification results show that the proposed scheme can effectively improve the power quality of the grid-connected point of air conditioning load in flexible-recovery mode, and enhance system stability in the multi-mode air conditioning load recovery scenario.

Acknowledgement

This work was supported by the Science and Technology Project of the State Grid Corporation of China (No. 5400-202340383A-2-3-XG).

References

[1] Y. Hou, L. Zhao, H. Jiang, X. Ji and J. Zhao, "Two-Layer Control Framework and Aggregation Response Potential Evaluation of Air Conditioning Load Considering Multiple Factors," *IEEE Access*, vol. 12, pp. 34435-34451, 2024.

[2] L. Su, R. Lyu, H. Guo, Y. Cai and Q. Chen, "Coordinating Air Conditioning Load Clusters to Provide Frequency Regulation Using Setpoint Changes," *2024 7th International Conference on Energy, Electrical and Power Engineering (CEEPE)*, Yangzhou, China, pp. 905-910, 2024.

[3] Q. Lin, B. Wen, R. Burgos, X. Li, Q. Wang and X. Li, "D-Q Impedance Modeling and Stability Analysis of a Three-Phase Four-Wire System With Single-Phase Loads," *IEEE Transactions on Power Electronics*, vol. 38, no. 9, pp. 11169-11182, Sept. 2023.

[4] Y. Li, J. He, Y. Liu, Y. Ren and Y. W. Li, "Decoupled Mitigation Control of Series Resonance and Harmonic Load Current for HAPFs With a Modified Two-Step Virtual Impedance Shaping," *IEEE Transactions on Industrial Electronics*, vol. 70, no. 8, pp. 8064-8074, Aug. 2023.

[5] C. -K. Lee, H. Liu, S. -C. Tan, B. Chaudhuri and S. -Y. R. Hui, "Electric Spring and Smart Load: Technology, System-Level Impact, and Opportunities," *IEEE Journal of Emerging and Selected Topics in Power Electronics*, vol. 9, no. 6, pp. 6524-6544, Dec. 2021.